Asian Journal of Chemistry; Vol. 36, No. 4 (2024), 851-858

ASIAN JOURNAL OF CHEMISTRY

https://doi.org/10.14233/ajchem.2024.30273


# Photocatalytic Degradation and Anticancer Activity of Green Synthesized Molybdenum Nanoparticles for Inhibiting the Cervical Cancer Cells

SANDHYA KUTIKANTI and SAVITA BELWAL*

Department of Chemistry, Anurag University, Hyderabad-500088, India

*Corresponding author: E-mail: saovita29@gmail.com

*Received*: 11 September 2023; *Accepted*: 23 February 2024; *Published online*: 30 March 2024; AJC-21582

This work reports the synthesis of molybdenum nanoparticles (Mo NPs) through green routes using horse gram seed extracts and characterized by GC-MS, electronic (UV-visible) spectroscopy, IR, XRD and SEM techniques. Their potent applications as *in vitro* anticancer agent against HeLa cell lines and photocatalytic degradation of methyl orange (MO) and methyl violet (MV) dyes were also evaluated. The anti-malignant properties of Schiff base ligands [2-fluorobenzaldehyde semicarbazone ($L_1H$) and 2-fluorobenzaldehyde thiosemicarbazone ($L_2H$) with molybdenum metal precursor [dioxobis(2,4-pentanedionato)molybdenum] were also explored and their Mo complexes after conversion into nano form as both ligands, $L_1H$ and $L_2H$ approve their binding property based on molecular docking studies.

**Keywords: Green synthesis, Molybdenum nanoparticles, Antioxidant activity, Schiff base, Metal complexes, Anticancer activity.**

## INTRODUCTION

Nanotechnology has emerged as a powerful tool in many fields of science and engineering due to its focus on altering and enhancing materials on a nanoscale scale [1]. It is a fascinating domain to alter the materials in size, shape, morphology and dimensions, creating nanoparticles almost equal to the Bohr radius [2]. Green technology, which includes the employment of microorganisms like bacteria, fungi, yeast and plant material extract as a safe and eco-friendly tool for synthesizing nanoparticles, has taken the lead over physical and chemical methods [3,4]. Therefore, biogenic preparation of metal nanoparticles is extremely popular nowadays. Owing of existence of phytochemicals like flavonoids, terpenoids and quinines phenols, alkaloids and tannins plant-mediated synthesis has become a powerful unconventional instrument for synthesizing nanoparticles [5,6]. The phytonutrients are playing significant role in governing particle size *via* prompting and topographical reactions and performing role of capping agents [7].

Molybdenum has gained much attention owing to its wide-range applications [8,9]. Since molybdenum exist in various oxidation states and having low toxicity than other *d*-block elements thus, molybdenum nanoparticles are made to absorb, to cure many deficiency disorders. The deficiency may sometimes disrupt enzyme activity in nitrogen metabolism [10,11].

Molybdenum oxide derivatives due to their distinctive electrochemical and diverse topography is one of the captivating transition metal oxides [12]. Molybdenum oxide a verified chemical for various uses, primarily for Li-ion battery [13]. Still, a few reports have also used them to decontaminate water [14]. Even though several reports are available which are explaining the amazing photocatalytic activity of molybdenum trioxide ($MoO_3$) [15], though, few studies are there to examine the photocatalytic activity of $MoO_2$ [16]. Surface active ingredients are important tools to carve the morphological structure of nanoparticles, which in turn alters the property of material [17]. A little research support is there to describe the geomorphological controlled preparation of molybdenum oxide [18].

Of late, $MoO_3$ nanostructures display photocatalytic properties under UV-visible light. With the nanoparticles of $MoO_3$ under visible light, several applications have been explored and examined, such as photosensitive deterioration of methylene violet dye [19,20] and methylene orange dye [21], gas sensing properties [22], supercapacitor [23], oxidation of methanol [24], epoxidation [25], light/optical properties [26], lithium

storing capabilities [27]. The reduction property of $MoO_3$ in presence of light interconnects with the particles' chemical properties, shape and size. Several synthetic approaches have revealed two different phases (h- and α-phases) of $MoO_3$ [28]. Nanorod's morphologies were explained and exhibited the h-phase though another phase (a) resembles nanowires and plates [29,30]. In literature, many traditional electrode materials have been applied to eradicate harmful pollutants for sensor applications of $Fe_2O_3$, $Co_2O_3$, CuO, $TiO_2$ and molybdenum oxide, which are a few significant examples [31].

This research work summarizes our investigation in green synthesis, characterization and employment of new synthesized nanoparticles which were synthesized *via* ligands *viz*. 2-fluorobenzaldehyde semicarbazone ($L_1H$) and 2-fluorobenzaldehyde thiosemicarbazone ($L_2H$) with molybdenum metal precursor [dioxo*bis*(2,4-pentanedionato)molybdenum]. Owing to the distinctiveness in structure and diversity in application range, the ligands were chosen wisely for anti-malignant activity. Here we tried to explore the anti-malignant properties of the ligands and their Mo metal complexes after conversion into nano form. Since ligands $L_1H$ and $L_2H$ approve their binding property based on theoretical study *i.e.* molecular docking, thus all the nanoparticles were tested against HeLa cell line in *in vitro*.

## EXPERIMENTAL

The starting materials procured through Sigma-Aldrich Company, were utilized as such without purification, while the solvents were dehydrated, dried and distilled by standard methods. Ligands [2-{1-(2-fluorophenyl)methylene}]hydrazinecarboxamide ($L_1H$) and [2-{1-(2-fluorophenyl) methylene}] hydrazinecarbothioamide ($L_2H$) were synthesized by [2-{1-(2-fluorophenyl)methylene}] with semicarbazide and thiosemicarbazide, dissolved in ethyl alcohol in 1:1 ratio (**Scheme-I**). The contents were refluxed for 5-6 h. The solid mass was filtered, washed with ethanol, recrystallized and dired over fused $CaCl_2$ under a vacuum.

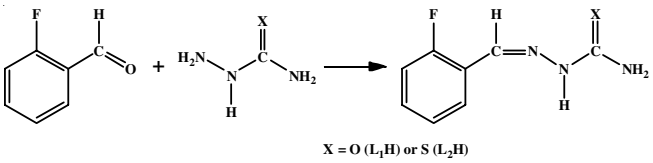


X = O ($L_1H$) or S ($L_2H$)

**Scheme-I**

Molybdenum complexes were synthesized by the addition of aqueous ethyl alcohol solution of $[MoO_2(acac)_2]$ dioxobis-(2,4-pentanedionato)molybdenum to a hot solution of $L_1H$ and $L_2H$ in 1:2 molar ratio with empirical formula $MoC_{16}H_{14}N_6O_4F_2$ and $MoC_{16}H_{14}N_6O_2S_2F_2$, respectively. The obtained solid products were washed with hot distilled water followed by aqueous ethnol and finally recrystallized. TLC technique was employed to test the purity of reaction products (**Scheme-II**).

**Seed extract preparation:** Horse gram seeds with brown coats were purchased from the local supermarket, washed them with water, sterilized them with 0.1% $HgCl_2$ to remove dirt and other impurities, soaked them in distilled water for 12 h at 4 ºC,

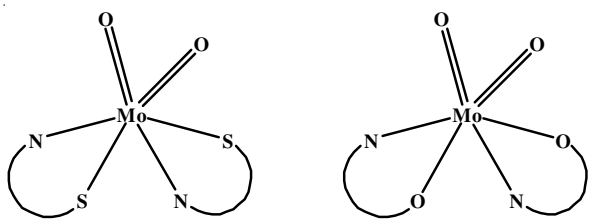


**where, N S and N O represent the donor system of ligand moiety**

**Scheme-II:** Mo(VI) complexes with ligands $L_1H$ and $L_2H$

allowed them to germinate for 48 h at 30 ºC, humidified frequently by using deionized water by for about 11-12 h. A thick paste was made by grinding dry sprouted seeds with tris buffer and phosphate buffer solutions (pH 8). The resulting mixture was filtered through double layer of filter paper and the filtrate was allowed centrifuge at 12000 rpm for 6-8 min below 4 ºC and collect the supernatant liquid, collected extract solution analyses for gas chromatography-mass spectrum.

**Synthesis of Mo nanoparticles by plant extract:** Horse gram seed extracts, a substantial volume of solution, were added to a crucible containing a definite volume of metal salt solution (1:4) and then heated at 60-70 ºC by continuous stirring for about 1 h; colour change was observed. The change of colour from yellow to brown indicates the conversion of metal ions into molybdenum nanoparticles (Mo NP), then the NPs was collected *via* centrifugation and drying [32].

The synthesized nanoparticles were analyzed by electronic (visible) and infrared spectroscopy. Size and crystallinity were identified by X-ray diffraction studies, further size was calculated by Debye-Scherrer equation. Further, the nanoparticles were examined by SEM to get an idea about their size, shape and surface morphology. These nanoparticles were further characterized for their cytotoxic activity through molecular docking and in *in vitro* studies.

**GC-MS data:** The extract was analyzed using Averin Biotech, Hyderabad (India) with CMMFT-RUSA-2.0 GCMS spectrometer. Using standard protocols of GC-MS, the biochemicals such as protein, amino acid, antioxidants, alkaloids, phenolic phytochemicals and several biologically important molecules were identified.

**Photocatalytic activity:** Methyl orange and methyl violet dyes were selected to estimate the light sensitized catalytic property of newly synthesized nanoparticles and evaluated with standard literature method [33]. A 1 ppm solution of methyl orange and methyl violet dyes was prepared in distilled water. On the other hand, different concentrations of all nanoparticles (10, 15, 20 ppm) were prepared and added to the conical flasks of both dyes. All the solutions were exposed to white light at 200 rpm for around 3-4 h. After every 20 min, 5 mL from flask was collected and the concentrations of dyes were analyzed by UV-visible spectrophotometer. For this experiment, the $\lambda_{max}$ value for methyl orange and methyl violet dyes were 470 and 610 nm, respectively. The degradation of dyes was analyzed by using following formula:

$$\text{Degradation (\%)} = \frac{A_0 - A}{A_0} \times 100$$

**Anticancer activity:** Cancer cell lines were procured from NCCS, Pune, India and contained in DMEM, augmented with 10% FBS (fetal bovine serum) and penicillin/streptomycin (0.5/mL) at 35-36 ºC in $CO_2$/air (5:95%). The cancer cell lines were placed in 96-well plates at $5.0 \times 10^3$ cells per well in 100 µL medium and kept overnight at 32-40 ºC for incubation to evaluate the MTT assay [34]. To explore the cell viability, the experiment was performed in triplicate with six concentrations of test compounds (5-100 µg/mL). After every 24 h of incubation, the treatment was taken out and fresh media was added. Further, to each well new media with MTT solution was added and the old test sample was discarded. The plates were kept in incubator around 35-37 ºC at least for 3-4 h. The measurement of absorbance of crystals soluble in DMSO was analyzed at wavelength 560 nm.

$$\text{Inhibition (\%)} = 100\frac{\text{Control} - \text{Treatment}}{\text{Control}}$$

## RESULTS AND DISCUSSION

**GC-MS studies:** The GC/MS spectrum of *Macrotyloma uniflorum* seed extract (Fig. 1) showed 20 to 25 peaks which specifies the presence of several key phytochemical compounds. The name of chemical compounds, molecular weight and retention times are reported in Table-1. Several other phytochemicals were identified through GC/MS profile of horse gram seed extract, were approximately comparable to the reported literature [35].

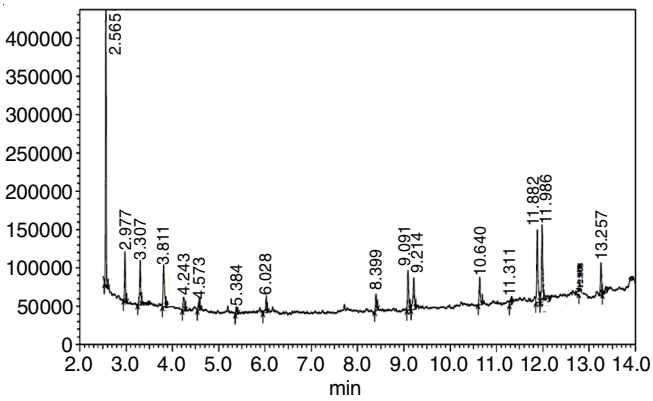


Fig. 1. GC-MS chromatogram of *Macrotyloma uniflorum* extract

TABLE-1
GC-MS DATA OF PHYTOCHEMICALS IN THE *Macrotyloma uniflourum*

| Retention time | Compound | m.f. | m.w. |
|---|---|---|---|
| 10.640 | Hexadecane | $C_{16}H_{34}$ | 226 |
| 14.11 | Hexadecane, 2,6,10,14-tetramethyl | $C_{20}H_{42}$ | 282 |
| 15.274 | heptadecane, 2,6,10,15-tetramethyl | $C_{21}H_{44}$ | 296 |
| 18.283 | Dibutyl phthalate | $C_{16}H_{22}O_4$ | 278 |
| 16.066 | Eicosane | $C_{20}H_{42}$ | 282 |
| 17.718 | Tritetracontane | $C_{34}H_{70}$ | 478 |
| 15.97 | Octadecanoic acid, | $C_{18}H_{36}O_2$ | 284 |
| 14.457 | Heptadecane | $C_{17}H_{36}$ | 240 |
| 14.965 | Octadecane, 5-methyl- | $C_{19}H_{40}$ | 268 |
| 15.750 | 3,5-Dimethylthiophenol, | $C_{11}H_{18}SSi$ | 210 |

**Electronic studies:** The synthesized molybdenum nanoparticles were exposed to UV-visible light to study the electronic spectroscopy. The absorption bands ($\lambda_{max}$) for both metal nanoparticles observed around 250-300 nm, which falls under the UV-C region [36] (Fig. 2). This region is called the short-wave ultraviolet region, which ranges from 200-280 nm. This ability due to unique phenomenon SPR (surface plasmon resonance) [37]. Study shows that molybdenum nanoparticles, after absorbing UV-Vis rays, exhibit nanosensors property and photocatalytic activity.

**FTIR studies:** The IR spectrum of ligands ($L_1H$ and $L_2H$) show peaks around 3340 $cm^{-1}$ for –NH *str.*, 1593 $cm^{-1}$ for C=N, 1691 $cm^{-1}$ for –C=O, 873 $cm^{-1}$ for –C=S and twin peaks ranges from 3471-3281 $cm^{-1}$ for $–NH_2$ groups (Fig. 3). The FTIR of MNPs show the functional groups and bonds present in the compounds ($ML_1$ and $ML_2$). In Fig. 4, the peaks were observed at 466, 1153, 1388, 1748, 2355 and 2924 $cm^{-1}$. The band around 466 $cm^{-1}$ is broad and significant peak below 1100 $cm^{-1}$ [38]. The peaks at 466, 520 and 607 $cm^{-1}$ are expected to be the Mo-O, Mo-N and Mo-S stretching, respectively.

**XRD studies:** The X-ray diffraction spectra of MoNPs prepared by reducing Mo metal complexes with horse gram seed extract were analyzed. The diffraction peaks were observed at 2θ values 82.45º, 19.48º and 8.85º for Mo NPs prepared from $ML_1$ complex. Likewise, five different peaks were also observed at 2θ values 27.30º, 24.14º, 23.20º, 14.61º, 11.35º of XRD patterns of Mo NPs prepared from $ML_2$ complex (Fig. 5).

Debye-Scherrer's equation was used to determine the average crystallite size of the green synthesized Mo NPs.

$$D = \frac{K\lambda}{\beta\cos\Phi}$$

where K = constant, λ = wavelength of X-rays and β = FWHM.

**SEM studies:** The SEM images display the spherical shape of the synthesized Mo NPs using a green method and found to be the range of 19-20 nm as determined from X-ray diffraction (XRD) data. The images (Fig. 6) also indicate the uneven and asymmetrical arrangement of green nanoparticles.

**Photocatalytic studies:** The analysis of the photocatalytic activity revealed a gradual reduction in the concentration of both methyl orange (MO) and methyl violet (MV) dyes due to the influence of nanoparticles. The results are influenced by the period of time and concentration of nanoparticles. The Mo NPs exhibited higher efficacy at 15 ppm synthesized from the $ML_2$ complex demonstrating superior performance compared to the other synthesized nanoparticles. The nanoparticles synthesized from $ML_2$ complex achieved degradation percentages of 82% for MO and 75% for MV after being exposed to UV light for 2 h. Whereas Mo NPs synthesized from $ML_1$ complex exhibited degradation efficiency of 73% for MO dye and 70% for MV dye. A bar diagram (Fig. 7) summarizes the photocatalytic activity of all nanoparticles prepared from horse gram seed extract. The photocatalytic activity is believed to be driven by reactive oxygen species (ROS) like superoxide anion ($O_2^{\bullet-}$), hydroxyl radical ($^{\bullet}OH$) and $H_2O_2$ as indicated in previous studies [39].

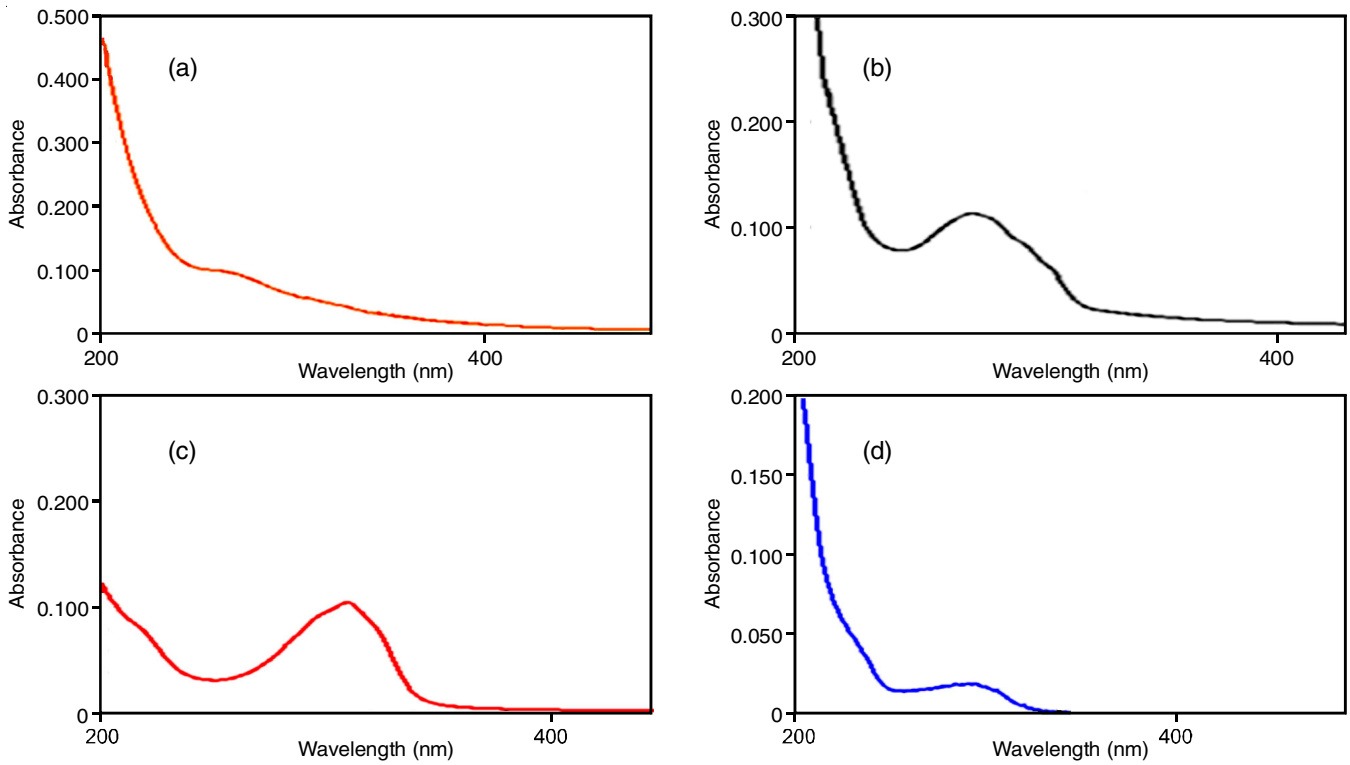


Fig. 2. Electronic spectra of (a) $L_1H$, (b) $L_2H$, (c) $ML_1$, (d) $ML_2$

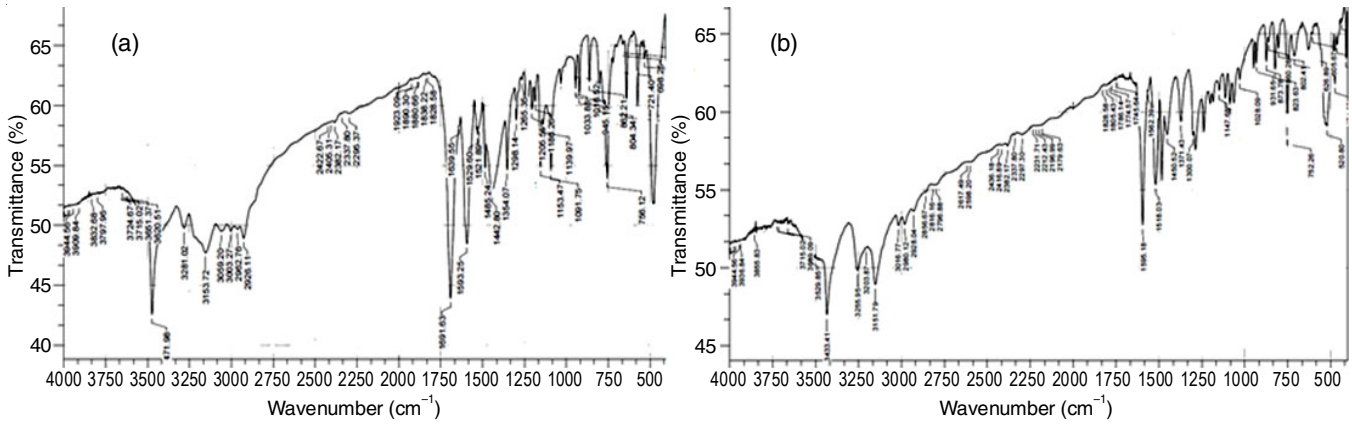


Fig. 3. IR spectra of NPs (a) $L_1H$ (b) $L_2H$

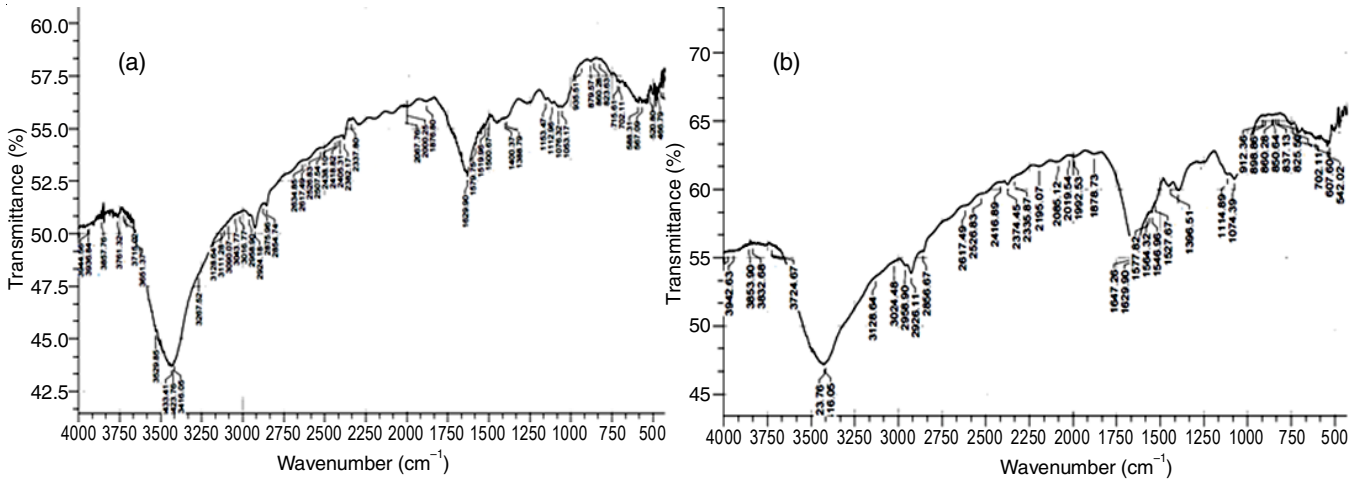


Fig. 4. IR spectra of NPs (a) $ML_1$ (b) $ML_2$

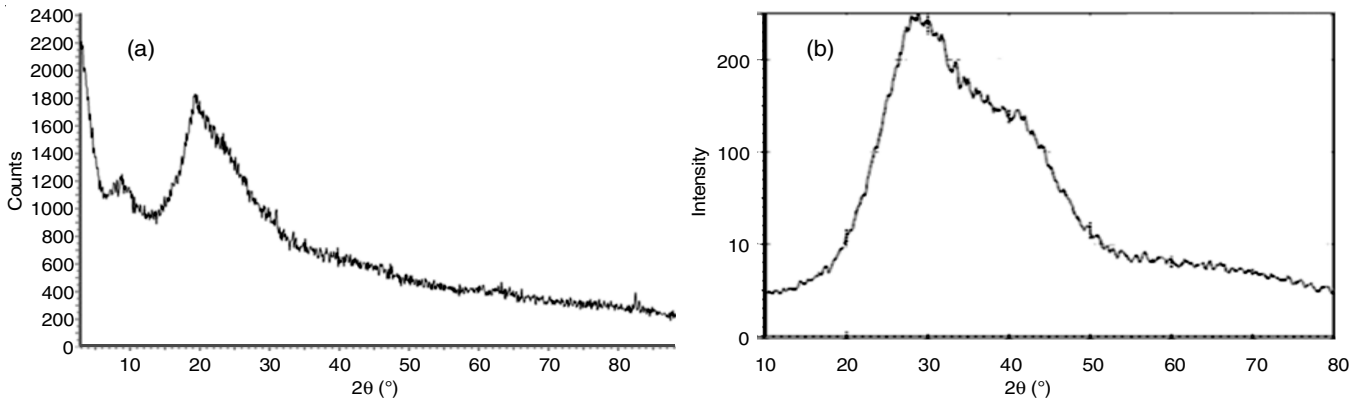


Fig. 5. XRD spectra of (a) Mo-NPs $ML_1$ and (b) Mo-NPs $ML_2$

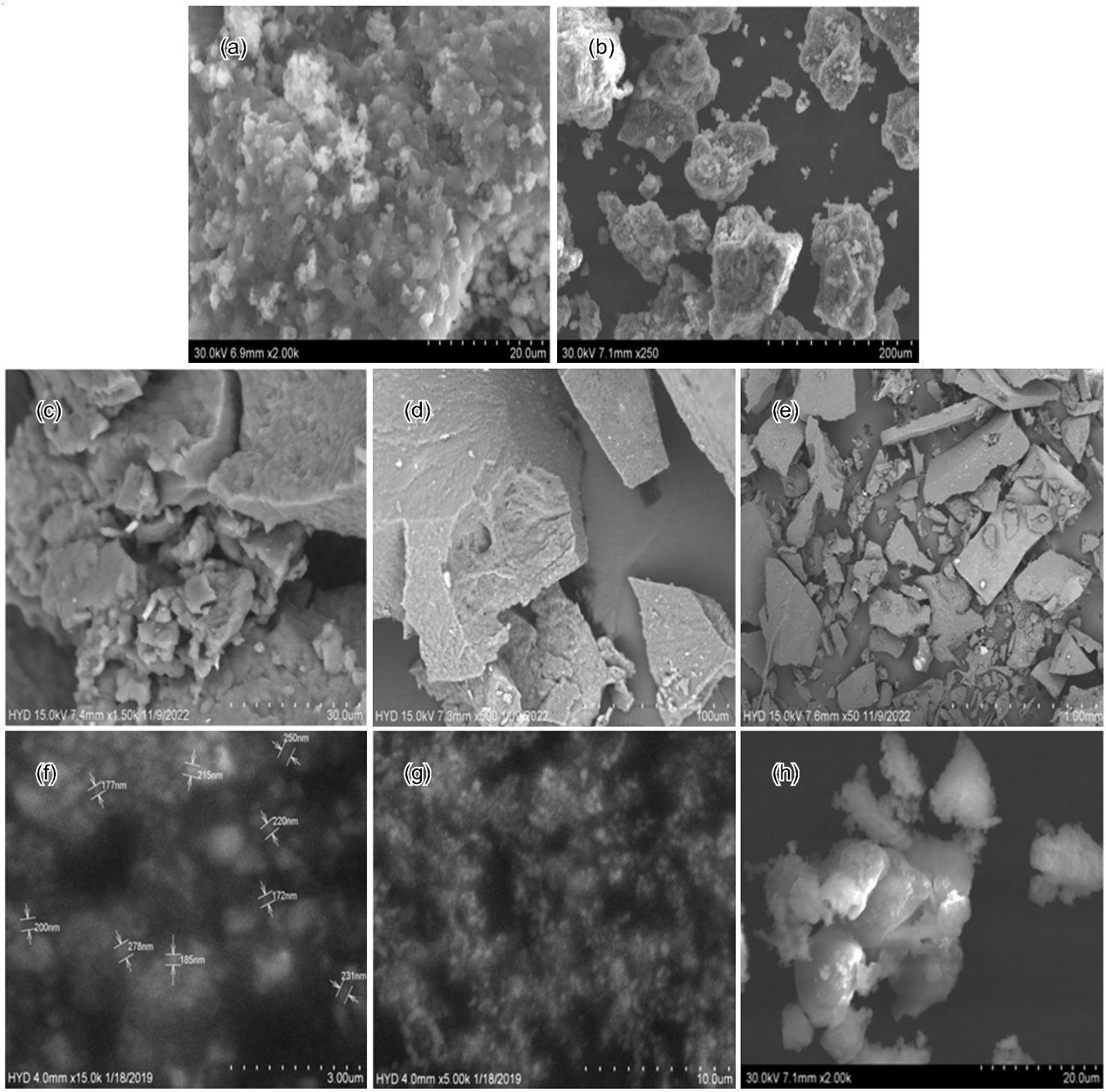


Fig. 6. SEM images of (a) $L_1H$, (b) $L_2H$, (c-e) $ML_1$ and (f-h) $ML_2$

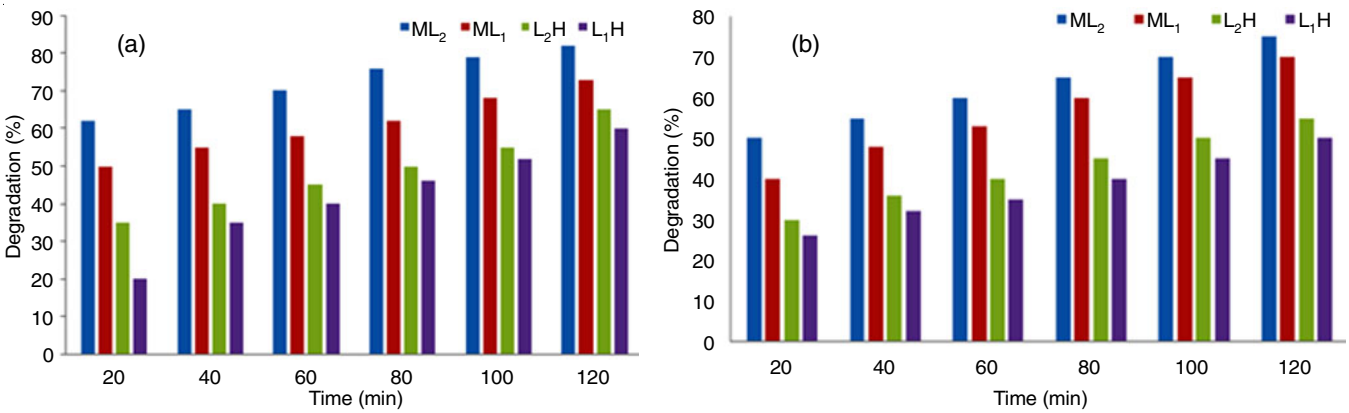


Fig. 7. Bar graphs showing photocatalytic activity of all NPs with (a) methyl orange and (b) methyl violet dyes

**Molecular docking studies:** Molecular docking study were performed using LibDock to study analyze the selected complex binding approach and affinity with modeled RAT nitric oxide synthase of brain protein. Based on the LibDock score and extremely interrelating amino acid residues, the finest ligand conformation was selected. Rutin exhibits the highest LibDock score of 119.72 Kcal/mol and binding affinity among the 10 conformations generated for each complex. The interaction analysis of H-bonding affinity with nitro-L-arginine methyl ester shows 90.235 Kcal/mol. Apart from rutin and other compounds, hesperidin also shows good binding affinity to LibDock score count 112.331 Kcal/mol (Table-2). In this work, we have analyzed compounds based on selected target proteins for their anti-malignant activity through molecular docking study [40]. The binding interaction of complexes $L_1H$ and $L_2H$ with the target protein was confirmed using docking results, indicating significant interactions and implying their inhibitory effect (Fig. 8). This study suggests that compounds $L_1H$ and $L_2H$ could potentially inhibit RAT nitric oxide synthase in brain proteins related to growth and may serve as a therapeutic drug.

**Anticancer activity:** Evaluation of cell viability for green synthesized Mo NPs was performed using MTT assay against HeLa cancer cell lines. The cell viability of the cancer cell depends on the dosage of the compounds. The results were compared with the standard cisplatin; the $IC_{50}$ value of cisplatin against the HeLa cell line was found to be 3.58 µg/mL. Among the four complexes, $ML_2$ complex exhibits the most significant

TABLE-2
DOCKING SCORES OF THE COMPOUNDS WITH MODELED RAT NITRIC OXIDE SYNTHASE OF BRAIN PROTEIN

| Name of the molecule | C docker energy | -c docker interaction energy | Interacting amino acids | Interacting atoms | H-Distance |
|---|---|---|---|---|---|
| Ligand 1 $L_1H$ | 30.259 | 32.722 | DG12, DT10, Asn722, Thr718, TGp11, Asp533, Arg364, DA113, Dc112 | A: ARG364: HH22 - Ligand1: O13 | 1.831000 |
| Ligand 2 $L_2H$ | 48.512 | 58.769 | DG12, DT10, Asn722, Thr718, TGp11, Asp533, Arg364, DA113, Dc112 | A: THR718: HG1 - Ligand2: F7<br>Ligand2: H20 - A: ASP533: OD2<br>Ligand2: H19 - A: ASP533: OD2 | 2.307000<br>2.468000<br>2.222000 |

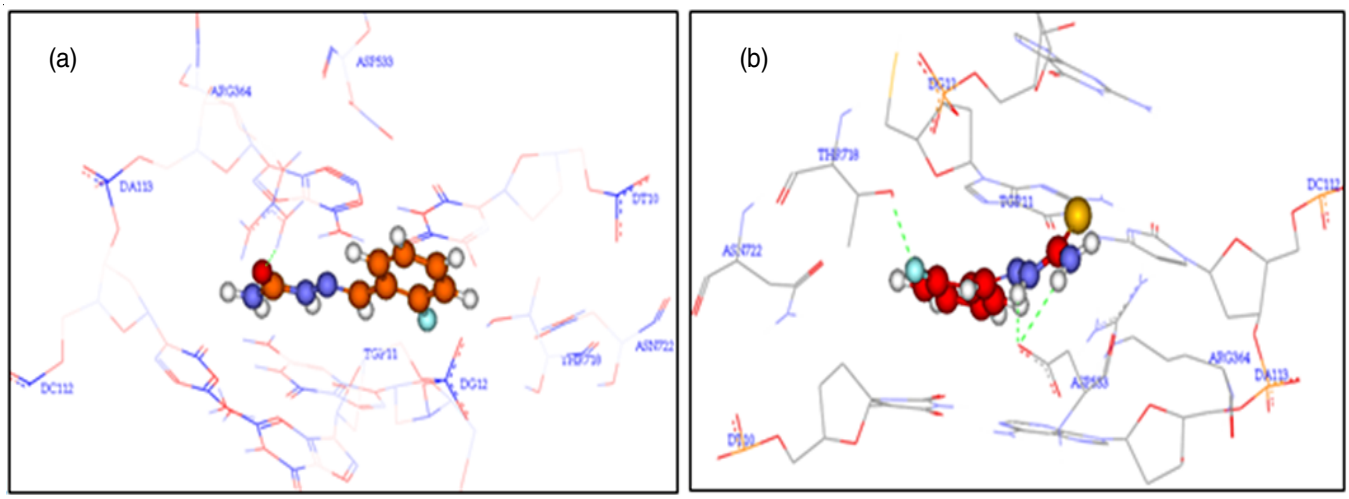


Fig. 8. H-bond interactions of (a) $L_1H$ and (b) $L_2H$. H-bond represented by green dotted lines and letters showing the amino acids involved in the bonding and compounds are shown by the boll model

toxicity to HeLa cells at 76.02 µm/mL. On the other hand, the molecular docking experiments have shown that the $L_2H$ ligand is more active than the $L_1H$ ligand. The comparative results of all four complexes with cisplatin suggests that all the complexes have shown moderate cytotoxicity and the percentage growth inhibition of the HeLa cell line increases as the concentration of the test compound increases.

## Conclusion

In this study, biogenic molybdenum nanoparticles (Mo NPs) were synthesized using horse gram seed extract and the phytochemical nutrients using GC-MS technique were analyzed. The green synthesized nanoparticles were evaluated for their antioxidant capabilities where the $ML_2$ complex had the lowest $IC_{50}$ value, indicating strong antioxidant activity. The photocatalytic experiment of methyl orange and methyl violet shows that degradation process depends on time and concentrations of Mo NPs. Amongst all nanoparticles, $ML_2$ based Mo NPs has shown highest photocatalytic efficiency. Furthermore, the MO NPs were also screened *in vitro* against HeLa cell line and the results were found to have moderate cytotoxicity.

## ACKNOWLEDGEMENTS

The authors extend their appreciation and acknowledgement to the Averinbiotech Pvt. Ltd, Hyderabad, India, for providing their support.

## CONFLICT OF INTEREST

The authors declare that there is no conflict of interests regarding the publication of this article.

## REFERENCES

1. S.H. Baker, M. Lees, M. Roy and C. Binns, *J. Phys. Condens. Matter*, **25**, 386004 (2013); https://doi.org/10.1088/0953-8984/25/38/386004
2. H.P.T. Nguyen, S. Arafin, J. Piao and T.V. Cuong, *J. Nanomater.*, **2016**, 2051908 (2016); https://doi.org/10.1155/2016/2051908
3. A.K. Mittal, Y. Chisti and U.C. Banerjee, *Biotechnol. Adv.*, **31**, 346 (2013); https://doi.org/10.1016/j.biotechadv.2013.01.003
4. M. Owais, A. Chauhan, Tufail, Sherwani, M. Sajid, C.R. Suri and M. Owais, *Int. J. Nanomedicine*, **6**, 2305 (2011); https://doi.org/10.2147/IJN.S23195
5. R. Nair, S.H. Varghese, B.G. Nair, T. Maekawa, Y. Yoshida and D.S. Kumar, *Plant Sci.*, **179**, 154 (2010); https://doi.org/10.1016/j.plantsci.2010.04.012
6. K. Sreevani and V.V. Anierudhe, *J. Biomater. Tissue Eng.*, **12**, 1071 (2022); https://doi.org/10.1166/jbt.2022.3021
7. R. Javed, M. Zia, S. Naz, S.O. Aisida, N. Ain and Q. Ao, *J. Nanobiotechnology*, **18**, 172 (2020); https://doi.org/10.1186/s12951-020-00704-4
8. C.A. Ellefson, O. Marin-Flores, S. Ha and M.G. Norton, *J. Mater. Sci.*, **47**, 2057 (2012); https://doi.org/10.1007/s10853-011-5918-5
9. B.N. Kaiser, K.L. Gridley, J.N. Brady, T. Phillips and S.D. Tyerman, *Ann. Bot. Seman. Sch.*, **96**, 745 (2005); https://doi.org/10.1093/aob/mci226
10. G.P. Awasthi, S.P. Adhikari, S. Ko, H.J. Kim, C.H. Park and C.S. Kim, *J. Alloys Compd.*, **682**, 208 (2016); https://doi.org/10.1016/j.jallcom.2016.04.267
11. A. Kumar and G. Pandey, *Am. J. Nanosci.*, **3**, 81 (2017).
12. Z. Wei, Z. Hai, M.K. Akbari, D.C. Qi, K.J. Xing, Q. Zhao, F. Verpoort, J. Hu, L. Hyde and S. Zhuiykov, *Sens. Actuators B Chem.*, **262**, 334 (2018); https://doi.org/10.1016/j.snb.2018.01.243
13. X. Zhang, X. Song, S. Gao, Y. Xu, X. Cheng, H. Zhao and L. Huo, *J. Mater. Chem. A Mater. Energy Sustain.*, **1**, 6858 (2013); https://doi.org/10.1039/c3ta10399d
14. H. Hu, J. Xu, C. Deng and X. Ge, *Mater. Res. Bull.*, **51**, 402 (2014); https://doi.org/10.1016/j.materresbull.2013.12.056
15. A. Chithambararaj, N.S. Sanjini, A.C. Bose and S. Velmathi, *Catal. Sci. Technol.*, **3**, 1405 (2013); https://doi.org/10.1039/c3cy20764a
16. H.-M. Hu, J.-C. Xu, X.-Q. Ge, M. Sun, H. Xuan and K.-H. Zhang, *Wuji Huaxue Xuebao*, **30**, 60 (2014); https://doi.org/10.11862/CJIC.2014.060
17. R.B. Pujari, V.C. Lokhande, V.S. Kumbhar, N.R. Chodankar and C.D. Lokhande, *J. Mater. Sci. Mater. Electron.*, **27**, 3312 (2016); https://doi.org/10.1007/s10854-015-4160-3
18. X. Chen, Z. Zhang, X. Li, C. Shi and X. Li, *Chem. Phys. Lett.*, **418**, 105 (2006); https://doi.org/10.1016/j.cplett.2005.09.138
19. A. Bhaskar, M. Deepa and T.N. Rao, *ACS Appl. Mater. Interfaces*, **5**, 2555 (2013); https://doi.org/10.1021/am3031536
20. Y. Chen, X. Di, C. Ma, C. Zhu, P. Gao, J. Li, C. Sun and Q. Ouyang, *RSC Adv.*, **3**, 17659 (2013); https://doi.org/10.1039/c3ra42319k
21. W. Cho, J.H. Song, J.-H. Kim, G. Jeong, E.Y. Lee and Y.-J. Kim, *J. Appl. Electrochem.*, **42**, 909 (2012); https://doi.org/10.1007/s10800-012-0470-9
22. B. Guo, X. Fang, B. Li, Y. Shi, C. Ouyang, Y.-S. Hu, Z. Wang, G.D. Stucky and L. Chen, *Chem. Mater.*, **24**, 457 (2012); https://doi.org/10.1021/cm202459r
23. Y. Lei, J. Hu, H. Liu and J. Li, *Mater. Lett.*, **68**, 82 (2012); https://doi.org/10.1016/j.matlet.2011.10.043
24. S.H. Choi and Y.C. Kang, *ChemSusChem*, **7**, 523 (2014); https://doi.org/10.1002/cssc.201300838
25. J. He, H. Wang, C. Gu and S. Liu, *J. Alloys Compd.*, **604**, 239 (2014); https://doi.org/10.1016/j.jallcom.2014.03.134
26. Y. Liang, S. Yang, Z. Yi, X. Lei, J. Sun and Y. Zhou, *Mater. Sci. Eng. B*, **121**, 152 (2005); https://doi.org/10.1016/j.mseb.2005.03.027
27. Y. Liang, S. Yang, Z. Yi, J. Sun and Y. Zhou, *Mater. Chem. Phys.*, **93**, 395 (2005); https://doi.org/10.1016/j.matchemphys.2005.03.034
28. Y. Liang, Z. Yi, S. Yang, L. Zhou, J. Sun and Y. Zhou, *Solid State Ion.*, **177**, 501 (2006); https://doi.org/10.1016/j.ssi.2005.12.001
29. J. Liu, S. Tang, Y. Lu, G. Cai, S. Liang, W. Wang and X. Chen, *Energy Environ. Sci.*, **6**, 2691 (2013); https://doi.org/10.1039/c3ee41006d
30. S. Liu, H. Yin, H. Wang, J. He and H. Wang, *Ceram. Int.*, **40**, 3325 (2014); https://doi.org/10.1016/j.ceramint.2013.09.102
31. N.P. Shetti, S.D. Bukkitgar, K.R. Reddy, C.V. Reddy and T.M. Aminabhavi, *Colloids Surf. B Biointerfaces*, **178**, 385 (2019); https://doi.org/10.1016/j.colsurfb.2019.03.013
32. K.M. Mamatha, V. Srinivasamurthy, C.R. Ravikumar, H.C.A. Murthy, V.G.D. Kumar, A.N. Kumar and A.A. Jahagirdar, *Sensors Int.*, **3**, 100153 (2022); https://doi.org/10.1016/j.sintl.2021.100153
33. A.R. Khataee and M.B. Kasiri, *J. Mol. Catal. Chem.*, **328**, 8 (2010); https://doi.org/10.1016/j.molcata.2010.05.023
34. A. Venkanna, B. Siva, B. Poornima, P.R. Rao Vadaparthi, K.R. Prasad, K.A. Reddy, G.B.P. Reddy and K.S. Babu, *Fitoterapia*, **95**, 102 (2014); https://doi.org/10.1016/j.fitote.2014.03.003

35. R. Dandekar, B. Fegade and V.H. Bhaskar, *J. Pharmacogn. Phytochem.*, **4**, 148 (2015).
36. H. Cheng, T. Kamegawa, K. Mori and H. Yamashita, *Angew. Chem. Int. Ed.*, **53**, 2910 (2014); https://doi.org/10.1002/anie.201309759
37. H. Cheng, X. Qian, Y. Kuwahara, K. Mori and H. Yamashita, *Adv. Mater.*, **27**, 4616 (2015); https://doi.org/10.1002/adma.201501172
38. G.S. Zakharova, C. Täschner, V.L. Volkov, I. Hellmann, R. Klingeler, A. Leonhardt and B. Büchner, *Solid State Sci.*, **9**, 1028 (2007); https://doi.org/10.1016/j.solidstatesciences.2007.07.022
39. M.A. Awad, A. A. Hendi, K.M. Ortashi, B. Alzahrani, D. Soliman, A. Alanazi, W. Alenazi, R.M. Taha, R. Ramadan, M. El-Tohamy, N. Al-Masoud and T.S. Alomar, *Sens. Actuators A Phys.*, **323**, 112670 (2021); https://doi.org/10.1016/j.sna.2021.112670
40. R.V. Singh, R. Dwivedi and S.C. Joshi, *Transition Met. Chem.*, **29**, 70 (2004); https://doi.org/10.1023/B:TMCH.0000014487.86754.93